JOURNAL OF SYNCHROTRON RADIATION

ISSN 1600-5775

Received 27 November 2017
Accepted 1 February 2018

Edited by I. Lindau, SLAC/Stanford University, USA

Keywords: pump–probe experiments; UFXC32k; single-photon counting; pixel array detector; high frame rate.

Evaluation of the UFXC32k photon-counting detector for pump–probe experiments using synchrotron radiation

Anna Koziol,[a]* Michel Bordessoule,[b] Alessandra Ciavardini,[b] Arkadiusz Dawiec,[b] Paulo Da Silva,[b] Kewin Desjardins,[b] Pawel Grybos,[a] Brahim Kanoute,[b] Claire Laulhe,[b] Piotr Maj,[a] Claude Menneglier,[b] Pascal Mercere,[b] Fabienne Orsini[b] and Robert Szczygiel[a]

[a]Department of Measurement and Electronics, AGH University of Science and Technology, av. A. Mickiewicza 30, Kraków 30-059, Poland, and [b]Synchrotron SOLEIL, L'Orme des Merisiers, Saint-Aubin, BP 48, Gif-sur-Yvette Cedex, France. *Correspondence e-mail: ankoziol@agh.edu.pl

This paper presents the performance of a single-photon-counting hybrid pixel X-ray detector with synchrotron radiation. The camera was evaluated with respect to time-resolved experiments, namely pump–probe–probe experiments held at SOLEIL. The UFXC camera shows very good energy resolution of around 1.5 keV and allows the minimum threshold setting to be as low as 3 keV keeping the high-count-rate capabilities. Measurements of a synchrotron characteristic filling mode prove the proper separation of an isolated bunch of photons and the usability of the detector in time-resolved experiments.

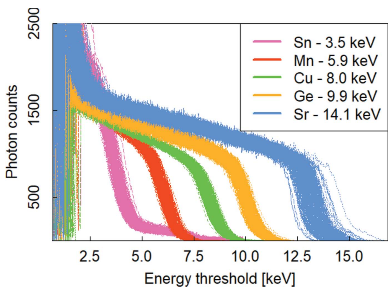

1. Introduction

Radiation produced by the synchrotron storage ring is characterized by its pulsed temporal structure which consists of high-frequency series of photon bunches. With a specific filling mode of the storage ring it is possible to isolate a single X-ray pulse from the rest of the storage ring, *e.g.* so-called hybrid or single-bunch filling modes. These specific pulsed modes are used to perform time-resolved experiments.

At the SOLEIL synchrotron time-resolved diffraction experiments are implemented by following a pump and probe scheme implemented at the CRISTAL hard X-ray beamline (Laulhé *et al.*, 2012). In a pump–probe experiment, the studied sample is subjected to very short infrared laser pulses of $\sim$40 fs duration. The laser pulses induce transient changes in the sample's atomic structure on timescales that can be as short as a few tens of femtoseconds. The objective of the experiment is to describe such changes and the dynamics of the crystal by performing experiments in the time domain.

In a classical pump and probe scheme (Polli *et al.*, 2007) the sample is excited by a laser pulse and probed after a certain delay Δt by a single pulse of synchrotron X-rays. The resulting diffraction pattern is recorded with a two-dimensional pixel detector. In order to generate statistically valuable information necessary for a reliable measurement, the pump and probe process must be repeated in a stroboscopic way. As a consequence, this technique can only be applied to measure reversible dynamical processes, which can be triggered periodically with the laser pulse (the relaxation time of the sample must be shorter than the laser repetition period).

This paper proposes an improvement to this classical scheme based on probing the sample's response twice at two different pump–probe delays after each laser excitation. The first measurement taken after a short delay allows study of the photo-induced dynamics. The second one, taken at half the period of laser repetition, when the sample relaxation is complete, is a reference measurement which permits detection and the compensation of drifts in the experimental conditions (*e.g.* beam misalignment, sample degradation *etc.*).

This requires a detector with very specific characteristics. First of all, in order to select photons from an isolated bunch, it must be able to count on demand for periods of time no longer than ~150 ns (gateable operation). Furthermore, gating frequency must be twice the laser repetition rate in order to probe the sample's response twice. Currently, the maximum laser repetition rate at the CRISTAL beamline is 1 kHz but in the near future it will reach 5 kHz. Therefore, the gate frequency must be at least 10 kHz to fulfil the pump and probe–probe requirement. Other detector requirements are:

(i) Large detection efficiency: 7–25 keV – CRISTAL beamline energy range.

(ii) Two counters and two thresholds per pixel – either energy discrimination or pileup detection at high photon fluxes.

(iii) High frame rate – at every probe (or gate) two images that correspond to two thresholds will be read out. Therefore, at a laser repetition rate of 5 kHz, the detector must be capable of operation at 20000 frames per second.

(iv) Fast signal processing to avoid saturation in the front-end electronics.

(v) Energy resolution that allows operation with the working photon energy of 7 keV.

There are several state-of-the-art X-ray detectors working either in charge integration (Henrich *et al.*, 2011; Ross *et al.*, 2016) or photon counting (Ejdrup *et al.*, 2009; Loeliger *et al.*, 2012) modes that are capable of gating isolated photon bunches and therefore of performing time-resolved experiments. However, only one of the detectors available today combines all the required characteristics, *i.e.* high frame rate, gated operation and energy discrimination. The detector able to fulfil all these requirements has been identified and proof-of-concept tests have already been performed and published by Dawiec *et al.* (2017). A comparison of the variety of pixel detector features is included in the work of Grybos *et al.* (2016).

This article is divided into three main sections: the first one describes the detector module, the second one the detector module characterization methods with the use of synchrotron radiation, and the third one presents the verification of a single-bunch isolation mode, proving that the detector module can indeed be used in a pump–probe–probe experiment.

2. Detector module based on UFXC32k ASIC

The UFXC32k (Grybos *et al.*, 2016) is a single-photon-counting hybrid pixel detector readout ASIC designed in 130 nm CMOS technology. Its matrix is built of 128 × 256 pixels, each of them with a square shape and a pitch of 75 µm. Every pixel is equipped with two independent discriminators with separate counters (called low and high) with a dynamic range up to 14 bits. When set in different configurations, the following operation modes are possible:

(i) Standard mode – two discriminators feed two counters independently and in parallel allowing photon counting in a given energy window.

(ii) High dynamic range mode – a single discriminator feeds one 28-bit counter, configured as two counters linked together.

(iii) Zero dead-time mode – a single discriminator feeds both counters alternately allowing photon counting in one counter during the readout procedure of the second one.

A schematic of a single pixel is shown in Fig. 1; it consists of a charge-sensitive amplifier (CSA), a shaper and two discriminators followed by two counters. The front-end electronics have a settable gain (high or low) which can be further adjusted with a 4-bit digital to analog converter (DAC). At the input of each discriminator, a 7-bit TrimDAC is implemented,

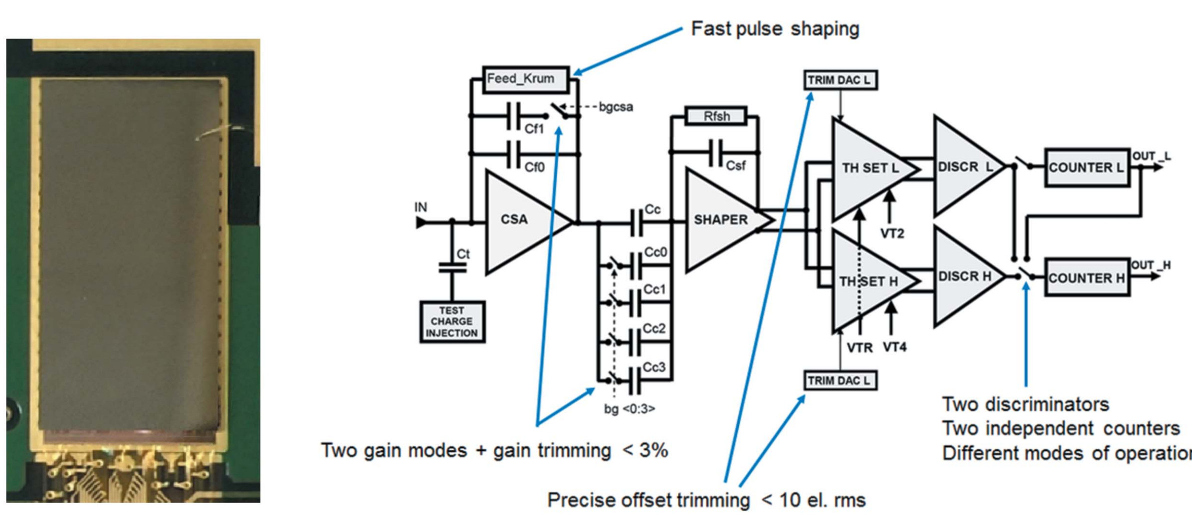

(*a*) (*b*)

Figure 1
Picture of a single chip detector module (*a*) and a single pixel architecture (*b*).

for threshold dispersion trimming. The discriminator level is set globally for both discriminators. The chip is capable of working at a high count rate depending on CSA Krummenacher feedback (Krummenacher, 1991) settings, which influences the noise (Ratti & Manazza, 2012; Kmon *et al.*, 2016). A dead time (Muller, 1988) of 85 ns can be obtained.

3. UFXC32k characterization with a synchrotron beam

All tests presented were performed at Synchrotron SOLEIL at the CRISTAL beamline. A hybrid pixel detector consisting of a single UFXC32k chip bump-bonded to a 320 µm-thick silicon sensor was used. The detector was exposed to synchrotron radiation operating in a hybrid mode, where an isolated electron bunch is in the middle of one empty quarter of the storage ring and a multi-bunch section spreads over the remaining three quarters. Symmetrical time gaps between the isolated bunch and the uniform sections are 147.64 ns.

Two setup configurations were used in the tests. Setup A was used to measure the energy resolution and detector linearity. Setup A is presented in Fig. 2(*a*). The detector was irradiated with a uniform beam as radiation was emitted from a fluorescence sample ionized by a synchrotron beam. The detector was placed at an angle of 90° to the direction of the synchrotron beam and 45° to the sample surface. The following fluorescence samples were used: Sn (3.5 keV), Mn (5.9 keV), Cu (8.0 keV), Ge (9.9 keV), Sr (14.1 keV).

Setup B was used to measure the high-count-rate capabilities of the detector. In setup B, the detector was placed on the direct beam path with its surface oriented perpendicularly to the beam direction, as shown in Fig. 2(*b*). The beam intensity was changed with the use of 16 removable aluminium foils with a thickness of 40 µm each, placed in front of the detector.

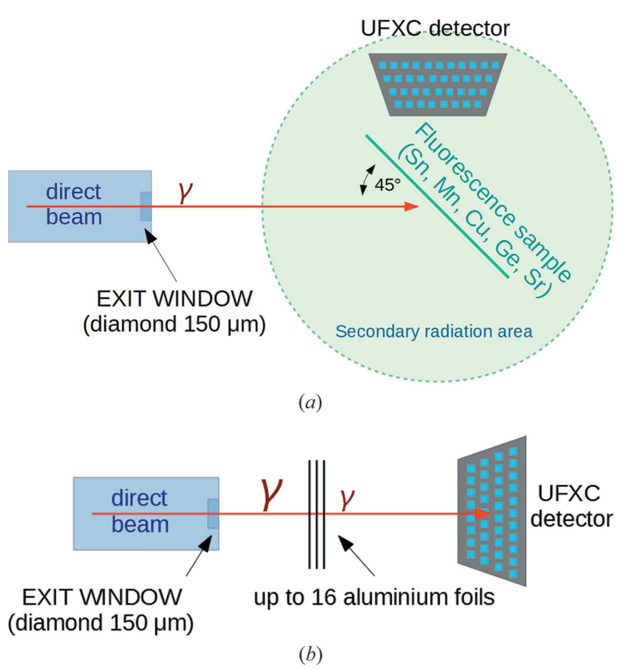

Figure 2
(*a*) Setup A for measurements with fluorescence radiation; (*b*) setup B for count-rate measurements.

With a double-crystal monochromator, a spectrum with one dominant 7 keV energy and its third harmonic, 21 keV, was obtained. As the beam was tight and had a Gaussian-shaped intensity profile, the analysed matrix area consisted of a non-uniformly illuminated area of 30 × 50 pixels.

The acquisition system was based on the NI PXI platform with a NI 7962R Kintex-7 FPGA, which also allows synchronization with synchrotron timing signals. The system was controlled by a *LabVIEW* program allowing data acquisition and analysis.

3.1. Energy gain

In order to minimize the effect of charge sharing (Chmeissani & Mikulec, 2001; Otfinowski, 2018), setting the threshold level at half of the photon energy is required (Kraft *et al.*, 2009). In order to set the threshold precisely, a very good trimming capability together with low noise and good energy resolution is essential. The UFXC32k has a unique way of threshold dispersion trimming, allowing a very high accuracy (Kmon *et al.*, 2016). Additionally, the gain dispersion can be minimized in the circuit to obtain a uniform response of all pixels to a photon of a given energy. For this purpose a fast correction algorithm (Maj, 2014), which reduces offset spread below 10 e^- r.m.s. (Grybos *et al.*, 2016), was used to trim the threshold dispersion, and the gain was trimmed using 9.9 keV fluorescence radiation using setup A. After correction, the gain dispersion value was reduced from 5.41% to 2.54% for the low discriminator and from 5.11% to 4.24% for the high discriminator.

The integral spectra after offset and gain trimming are presented in Fig. 3(*a*), showing a much improved response. The mean energy gain was calculated for each fluorescence sample. Fig. 3(*b*) shows the results together with linear models determined for the three lowest incident energies. As the experimental target energies can be as low as 3.5 keV, the high gain settings were used, resulting in a nonlinear response of the detector for energies exceeding 12 keV.

3.2. Minimum threshold setting

In addition to the low dispersions of both offsets and gain, the noise level of the detector defines the lowest possible energy threshold that can be applied in the experiment. To verify the lowest settable energy threshold with good separation from noise hits, an integral spectrum with an acquisition time of 1 s without X-ray radiation was collected. The results show that the minimum energy threshold level, for which less than ten noisy pixels in the whole matrix are observed, is about 3.0 keV (Fig. 4). The noisy pixels can be easily marked as so-called hot pixels and excluded from future analysis during the experiment.

3.3. Energy resolution

To estimate energy resolution of the detector, integral spectra were collected for all fluorescence samples in setup A. Fig. 5(*a*) shows the histograms of energy peak positions and a good separation between all energies is clearly visible. For

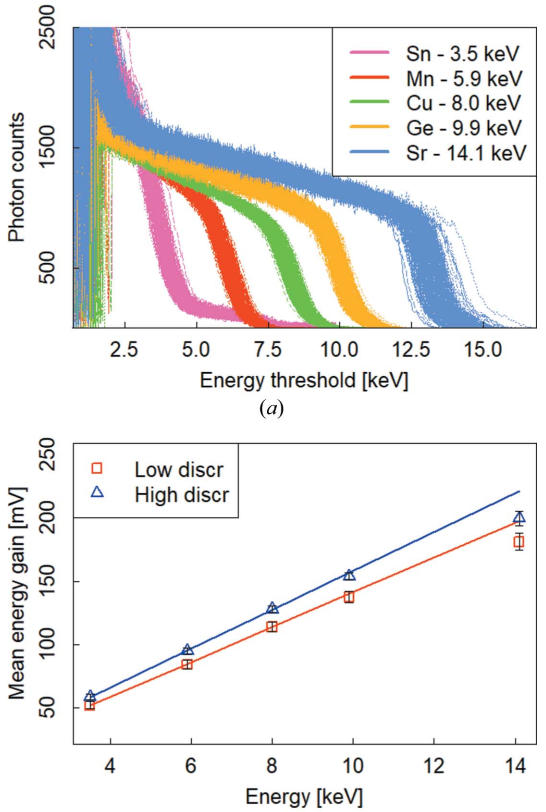

(*a*)

(*b*)

Figure 3
(*a*) Integral spectra for different incident energies. For easier data visualization, plots of only 3% of the randomly selected pixels are shown. (*b*) Gain linearity.

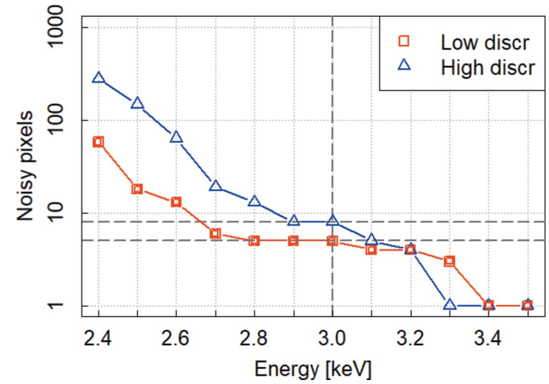

Figure 4
Number of noisy pixels at different energy discrimination levels.

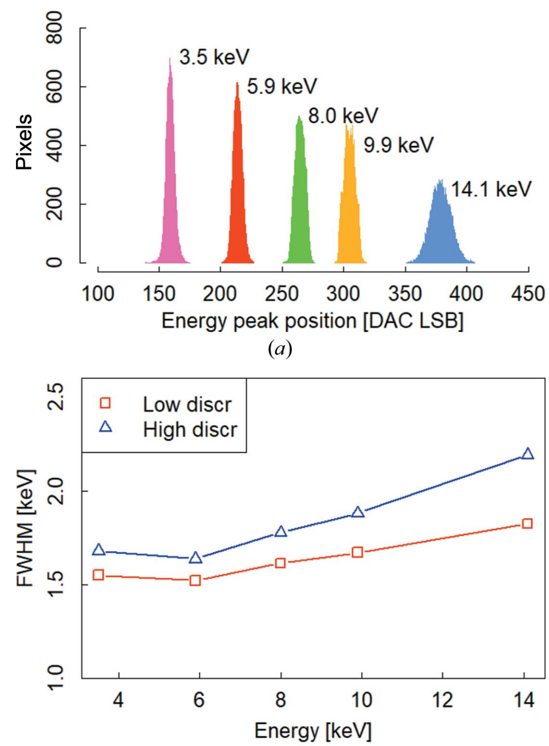

(*a*)

(*b*)

Figure 5
Histograms of energy peaks (*a*) and energy resolution (*b*).

each energy, integral spectra of every pixel were summed and divided by the number of pixels, giving a mean integral spectrum. This method is sensitive not only to noise but also to offset and gain spread among pixels. The obtained integral spectra were fitted using the S-curve extended by the charge-sharing effect contribution (Bergamaschi *et al.*, 2010). In Fig. 5(*b*) it is shown that energy resolution is better than 2.0 keV for energies below 14 keV. The presented result proves the usability of the UFXC32k hybrid pixel detector with photon energies from 7 keV required in the experiments.

3.4. High-count-rate capabilities

The results of time-resolved experiments depend greatly on the timing capabilities of the detector system. In the experiment, isolation of a single photon bunch is necessary and thus the gate should be opened for a time not longer than 150 ns. However, the total gate time consists of both the time of the gate open signal and the time of the discriminator output pulse width. For the 8 keV pulses, high gain settings and a threshold equal to half of the measured energy, the time of the discriminator high state equals about 30 ns, and so the time of the gate open signal can be set to about 120 ns.

The second issue related to high count rate is the capability of coupling with high radiation fluxes. As shown by Grybos *et al.* (2016), the dead time of the front-end is about 100 ns, which means that the front-end should recover from any saturation (if present) before the isolated bunch of photons arrives. Measurements to determine when the circuit can cope with high radiation fluxes were carried out using setup B. Fig. 6 shows the measured relation between the incoming number of photons and the number of photons registered by the UFXC32k detector. The result shows a linear response up to over 2×10^6 photons pixel^{-1} s^{-1}, which is more than expected for the pump–probe–probe experiments. It should be mentioned that the count-rate measurement has been performed using the isolated packets of photons; therefore for most of the time the detector was exposed to a much higher photon flux.

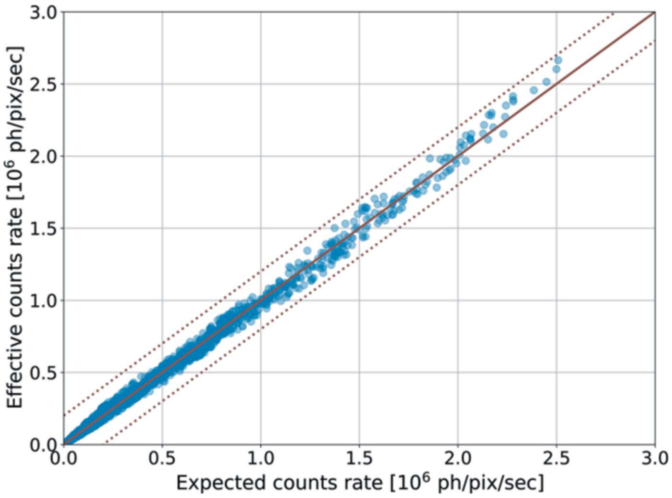

Figure 6
Count-rate measurement linearity.

4. Verification of the single photon bunch isolation

In order to verify the single photon bunch isolation, a mapping scan of the synchrotron ring filling mode (Dawiec *et al.*, 2017) was performed. The detector was operating in setup A with a photon energy of 7 keV and a gate time of 120 ns. The measurement was triggered each time at the same moment of the ring cycle with a different delay in the range of 0–1200 ns and with a 5 ns step. The data acquisition was repeated 10000 times at each delay to obtain statistically valuable information. The current per bunch during the measurements is shown in Fig. 7.

The scan was repeated with three different UFXC32k count-rate settings. Results for the single-bunch quadrant were analysed, and collected patterns, together with beam-integrated intensity calculations performed with the same parameters as the real measurement, are presented in Fig. 8.

As can be seen, the simulations match the measurements for all three count-rate settings of the detector. However, for

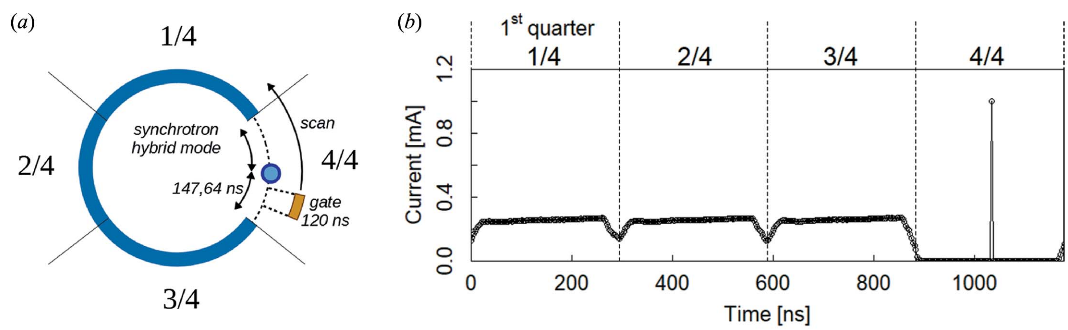

Figure 7
Schematic view of the SOLEIL hybrid filling mode with an isolated electron bunch in the middle of an empty quarter (*a*) and time distribution of current per electron bunch in the storage ring (*b*).

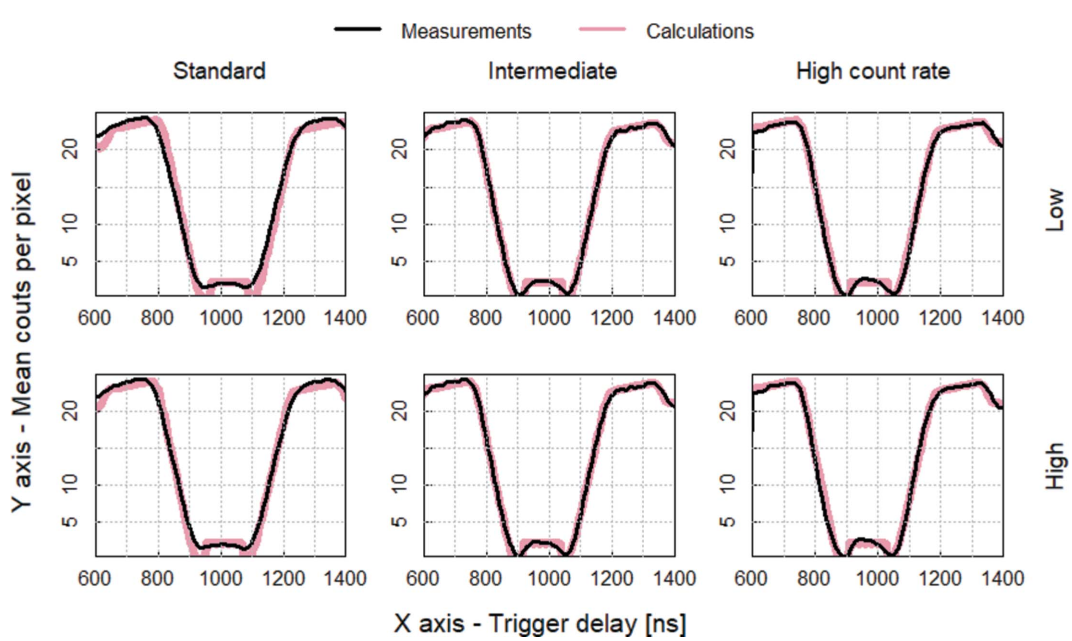

Figure 8
Single photons from an isolated electron bunch results for different chip count-rate settings.

the intermediate- and high-count-rate settings the separation of a single bunch is much better than for the standard one. This indicates that both discriminators are able to isolate photons from the single bunch at the SOLEIL synchrotron.

5. Summary

This article presents tools and methods used for hybrid pixel detector evaluation for a pump–probe–probe experiment. The presented results prove that the UFXC32k detector performance fulfils pump–probe–probe experiment requirements. It is possible to trim energy gain to 2.54% and set a minimum energy discrimination level as low as 3.0 keV. Therefore, it is very efficient in working with the 7 keV energy used at the CRISTAL beamline. The gain is linear in a large energy range and the energy resolution is less than 2 keV. Furthermore, the measured count-rate performance demonstrates linear operation up to 2×10^6 photons pixel^{-1} s^{-1} which is essential for time-resolved experiments. Additionally, the chip allows detection of single photons from the isolated electron bunch at SOLEIL. Although this work concentrates on the use of the detector at SOLEIL, it can be used at any synchrotron source with a filling mode that has a separation between an isolated bunch and the rest of the ring of at least 120 ns. The next step is to perform a pump–probe–probe experiment in real conditions with sample excitation by the laser. In parallel, a larger camera prototype dedicated to time-resolved studies will be developed.

Funding information

This work has been supported by the National Centre for Research and Development, Poland, PBS1/A3/12/2012, in the years 2012–2016, and by the National Science Centre, Poland, under contract No. UMO-2016/21/B/ST7/02228. Anna Koziol thanks the Ministry of Science and Higher Education in Poland for financial support.

References

Bergamaschi, A., Cervellino, A., Dinapoli, R., Gozzo, F., Henrich, B., Johnson, I., Kraft, P., Mozzanica, A., Schmitt, B. & Shi, X. (2010). *J. Synchrotron Rad.* **17**, 653–668.
Chmeissani, M. & Mikulec, B. (2001). *Nucl. Instrum. Methods Phys. Res. A*, **460**, 81–90.
Dawiec, A., Maj, P., Ciavardini, A., Gryboś, P., Laulhé, C., Menneglier, C. & Szczygieł, R. (2017). *J. Instrum.* **12**, C03057.
Ejdrup, T., Lemke, H. T., Haldrup, K., Nielsen, T. N., Arms, D. A., Walko, D. A., Miceli, A., Landahl, E. C., Dufresne, E. M. & Nielsen, M. M. (2009). *J. Synchrotron Rad.* **16**, 387–390.
Grybos, P., Kmon, P., Maj, P. & Szczygiel, R. (2016). *IEEE Trans. Nucl. Sci.* **63**, 1155–1161.
Henrich, B. *et al.* (2011). *Nucl. Instrum. Methods Phys. Res. A*, **633**, S11–S14.
Kmon, P., Maj, P., Grybos, P. & Szczygiel, R. (2016). *IEEE Trans. Nucl. Sci.* **63**, 1194–1201.
Kraft, P., Bergamaschi, A., Bronnimann, C., Dinapoli, R., Eikenberry, E. F., Graafsma, H., Henrich, B., Johnson, I., Kobas, M., Mozzanica, A., Schleputz, C. M. & Schmitt, B. (2009). *IEEE Trans. Nucl. Sci.* **56**, 758–764.
Krummenacher, F. (1991). *Nucl. Instrum. Methods Phys. Res. A*, **305**, 527–532.
Laulhé, C. *et al.* (2012). *Acta Phys. Pol. A*, **121**, 332–335.
Loeliger, T., Bronnimann, C., Donath, T., Schneebeli, M., Schnyder, R. & Trub, P. (2012). *IEEE Nucl. Sci. Symp. Conf. Rec.* pp. 610–615.
Maj, P. (2014). *J. Instrum.* **9**, C07009.
Muller, J. (1988). *A simple derivation of the Takacs formula*. Rapport BIPM 88/3. Bureau International des Poids et Mesures, Sèvres, France.
Otfinowski, P. (2018). *Nucl. Instrum. Methods Phys. Res. A*, **882**, 91–95.
Polli, D., Lüer, L. & Cerullo, G. (2007). *Rev. Sci. Instrum.* **78**, 103108.
Ratti, L. & Manazza, A. (2012). *IEEE Trans. Nucl. Sci.* **59**, 144–153.
Ross, S., Haji-Sheikh, M., Huntington, A., Kline, D., Lee, A., Li, Y., Rhee, J., Tarpley, M., Walko, D. A., Westberg, G., Williams, G., Zou, H. & Landahl, E. (2016). *J. Synchrotron Rad.* **23**, 196–205.